Equipment effects on dynamic properties of soils in resonant column testing

Soheil Moayerian, Lisa Katherine Reipas, Giovanni Cascante, Tim Newson
Department of Civil and Environmental Engineering
University of Waterloo / University of Western Ontario, Ontario Canada

2011 Pan-Am CGS Geotechnical Conference

ABSTRACT
The dynamic properties of a benchmark standardized laboratory sand (Ottawa silica sand) were evaluated with two different resonant column devices, utilising software with different analytical approaches for the evaluation of soil properties. The dynamic properties (shear modulus and damping ratio) are evaluated as a function of the shear strain level. The results are compared to evaluate the effect of the type of equipment and the form of the data analysis on the measured dynamic properties of the samples. The results are discussed in light of the applicability of the procedures in practice, the ease of the testing methods , and the errors they introduced into analysis and design. In general, the shear wave velocities obtained from the two different devices are in good agreement. However, the damping ratios they give show considerable differences as strains increase.

RÉSUMÉ
Les propriétés dynamiques d'un sable de laboratoire normalisées de référence(sable de silice d'Ottawa) ont été testés avec deux différents dispositifs colonne de résonance, en utilisant le logiciel avec les différentes approches analytiquespour l'évaluation de l'amortissement du matériel. Les propriétés dynamiques(module de cisaillement et le ratio d'amortissement) sont évalués en fonction du niveau de contrainte de cisaillement. Les résultats sont comparés pour évaluer l'effet de l'équipement et l'analyse des données sur les propriétés dynamiques mesurées sur les échantillons. Les résultats sont discutés à la lumière de l'applicabilité dans la pratique, la facilité de test, et l'effet des erreurs introduites dans l'analyse et de conception. En général, les vitesses des ondes de cisaillement obtenues par les deux appareils différents sont en bon accord.Toutefois, le ratio d'amortissement montre des différences plus importantes augrandes déformations.

1 INTRODUCTION

Shear modulus and damping ratio are important soil properties that influence the response of soils to dynamic loads. Both shear modulus and damping ratio can be evaluated in the laboratory using devices such as cyclic triaxial, bender elements (BE), or a resonant column device (RCD); which is the ASTM standard for dynamic characterization of soils (ASTM D4015-92 2000). The cyclic triaxial test is used for high shear strain levels ($>10^{-3}$), whereas bender elements and the RCD are used for low strain levels ($<10^{-3}$). Bender element tests are economical and fast; however, the results can be affected by many variables and they require careful interpretation ; On the other hand, BE can only be used to measure the shear modulus at low strain levels (G_{max}). The evaluation of material damping in the BE test is complex and there is no standard procedure (Camacho et al. 2008). The RCD provides more consistent test results; and it is considered one of the most accurate ways to determine the dynamic properties of soils at low to mid shear strain levels. Resonant column (RC) tests are accurate and reliable; however, the effect of different equipment in making the measurements on the results has not yet been evaluated. This is especially true of the damping measurements, which are significantly affected by the electromotive forces (EMF). (Cascante et al. 2003; Wang et al. 2003).

The RC tests can vary in their configuration and the analytical methods used for the computation of the dynamic properties. While many testing programs have been performed to measure the dynamic properties of soils on a single resonant column apparatus (Stokoe et al. 1994, Dobry and Vucetic 1987; Cascante and Santamarina 1997, Khan et al. 2005, Camacho et al. 2008), very few have evaluated the dynamic properties of the same soils on different RCDs. In most cases in which a soil was tested on two different RCDs the tests were for calibration purposes, when the RCD had been modified to accommodate different samples (e.g. stiffened base, Avramidis and Saxena 1990). In this case, however, the same test method and data analysis are used in the initial and modified state of the RCDs. Fewer comparisons have been done with two RCDs that use different testing methods and different data analysis. The main objective of this paper is to measure the dynamic properties of a typical silica sand using two different RCDs and provide a comparison of the results. The effect of the equipment and the use of different data analysis procedures for the calculation of damping are discussed.

2 BACKGROUND THEORY

Both of the RCDs used in this study have a similar general configuration, where the base of the sample is fixed and the applied torsional excitation is at the top of the sample as shown in Fig 1 (Stokoe type resonant column). The two devices are referred as RCD-1 and RCD-2. The RCD-1 is a custom-made device (Cascante et al. 2003); whereas the RCD-2 is a commercially available system (GDS-RCA, 2009). The primary differences between the two devices relate to their geometry, electronic components, and the data analysis procedures for calculation of the material damping ratio. This section provides a summary of the background theory used in both resonant column devices.

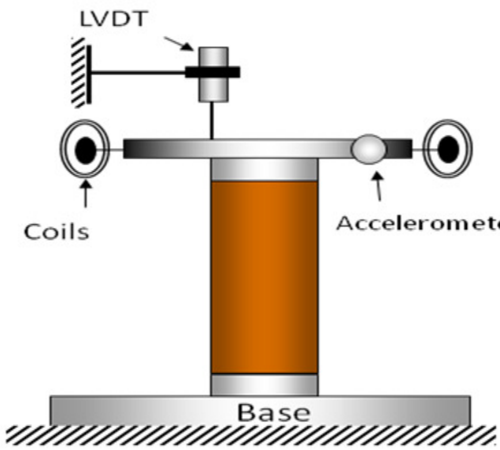

Figure 1. Basic schematic of fixed-free base resonant column device (Stokoe type).

The RCD-1 applies a sinusoidal chirp vibration with a wide range of frequencies to the soil specimen, and the resonant frequency is evaluated from the frequency response curve or transfer function of the system, which is represented as a single-degree-of-freedom system (SDOF). The input function is given by the applied torque (proportional to the current flowing through the coils); whereas the response function is given by the acceleration measured at the driving plate (Fig. 1). The damping ratio and the resonant frequency are determined by curve fitting the measured frequency response curve (Khan et al. 2008).

The instrumentation used in RCD-1 is illustrated in Figure 2. The input signal for the coils is generated by a built-in signal generator in a dynamic signal analyzer (HP-35670A). The low-power input signal is amplified by an audio power amplifier (Bogen 250W). The axial deformation of the specimen is measured with an LVDT (Schaevitz 500HR) mounted inside the resonant column device. The response of the specimen is measured with an accelerometer (PCB 353B65). The output signal of the accelerometer is monitored, processed, and stored in a digital oscilloscope (Agilent DSOX3014A), a dynamic signal analyzer (HP-35670A), and a computer. The cell and specimen pressures are controlled independently by a pneumatic pressure control panel (Brainard-Kilman E-400).

The applied torque is computed from the measured current passing through the coils $I_C(\omega)$ at a given angular frequency (ω), and the distance from the magnets from the center of the specimen (r_m). The experimentally measured magnetic coil factor (B_L) is used to convert current amplitude into torque amplitude as (Khan et al. 2008).

$$T_o(\omega) = B_L\, I_C(\omega)\, r_m \qquad [1]$$

The spectral angular rotation of the specimen ($\varphi(\omega)$) is computed from the spectral acceleration measurement ($\ddot{X}(\omega)$) on the driving plate at a distance (r_a) from the axis of the specimen as

$$\varphi(\omega) = \frac{\ddot{X}(\omega)}{\omega^2\, r_a} \qquad [2]$$

The phase lag between the torque and rotation is computed using the phase information from the cross-power Fourier spectrum of the input current and the output acceleration. The shear modulus and damping ratio as a function of frequency are computed by curve-fitting the transfer function between the applied torque, To(ω), and the induced angle of twist, φ(ω), given by (Khan et al. 2008)

$$\frac{T_o(\omega)\, e^{-i\phi(\omega)}}{\varphi(\omega)} = \left(I_o + \frac{I}{3}\right)\omega_o^{\,2}\left[1-\left(\frac{\omega}{\omega_o}\right)^2 + i\,2\,\xi\left(\frac{\omega}{\omega_o}\right)\right] \qquad [3]$$

where I is the mass polar moment of inertia of the specimen, Io is the mass polar moment of inertia of the driving plate, and ω_o is the resonant frequency. This equation considers that the damping ratio (ξ) to be frequency independent.

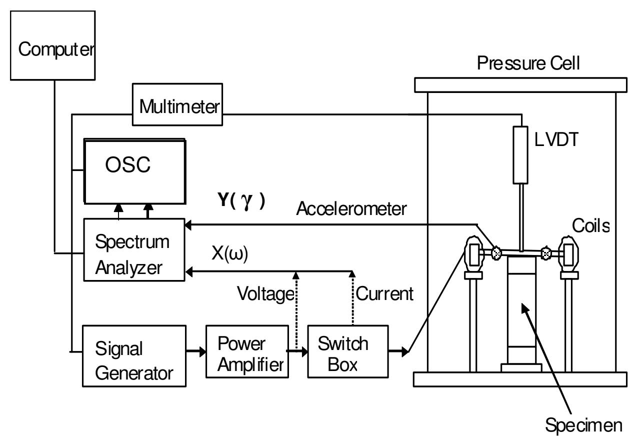

Figure 2. General instrumentation for resonant column device RCD-1

The RCD-2 uses conventional methods for evaluation of shear modulus and damping ratio as outlined in ASTM D4015-2007. The instrumentation used in RCD-2 is illustrated in Figure 3; whereas Figure 4 shows the driving plate system. The resonant frequency is assessed by applying different frequencies of excitation to the sample incrementally and selecting the frequency that corresponds to the maximum response in the measured frequency bandwidth. Once the resonant frequency is determined, the damping ratio is then computed using the free decay and the logarithmic decrement method. At the resonant frequency, the amplitude of twist (or rotation angle) approaches infinity for a zero damping material; thus, the solution for the equation of motion for fixed-free RC is given by (Richart et al. 1970):

$$\frac{I}{I_o} = \beta \tan \beta \quad [4]$$

where I is the mass polar moment of inertia of the specimen and $\beta = \omega H / V_S$. Equation 4 is used in conventional RC testing to compute the shear wave velocity (V_S) of the material. The shear modulus G (kPa) is calculated from shear wave (V_S) and the bulk density (ρ) of the specimen as $G = \rho (V_S)^2$. The standard analysis of resonant column results is then based on the continuum theory of elastic wave propagation; only when $I_0 >> I$ the fundamental frequency predominates and the approximation of a SDOF model can be used. Therefore to reduce data from the resonant column test, the mass polar moment of inertia of the drive system I_0 is required. As the drive system has a complex geometry, it is difficult to derive mathematically, its value is found experimentally. The mass polar moment of inertia of the specimen, I, is calculated from the mass (m) and the radius of the specimen (r) as $I = ½ m r^2$.

The damping ratio, (ξ), is computed from the shape of free vibration decay curve. First, a sinusoidal wave is applied at the resonant frequency of the specimen, and then the excitation is shut off so the resulting free vibrations may be measured. The free vibration response (*x(t)*) of a SDOF system is given as function of the phase angle (θ) and the initial amplitude (A_0) as (Richart et al. 1970)

$$x(t) = A_0 e^{-\xi \omega_0 t} \cos(\omega_D t + \theta) \quad [5]$$

where ξ is the damping ratio; ω_0, the circular resonant frequency; ω_D, the damped resonant frequency given by $\omega_D = \omega_0 \sqrt{1 - \xi^2}$; and A_0, the maximum amplitude of the displacement. For $\xi < 0.2$, $\omega_D \approx \omega_0$, whereas $\omega_D = 0.92\omega_0$ when ξ =0.4. The damping ratio can be estimated from the decrement logarithm method (Richart et al. 1970) as

$$\xi = \frac{1}{2\pi n} Ln\left(\frac{x(t_i)}{x(t_j)}\right) \quad [6]$$

where $x(t_i)$ and $x(t_j)$ are two peaks separated n cycles ($t_j = t_i + nT$). The full waveform of a free-decay response can be used to estimate a single value for the resonant frequency and damping ratio by curve-fitting the measured response with Eq. 5. The damping ratio is also calculated by plotting the Ln(peak amplitudes) against the phase angle (2π n). This plot should be straight line; and its slope represents the damping ratio. For the RCD-2, between 10 and 50 cycles are commonly used in the calculation.

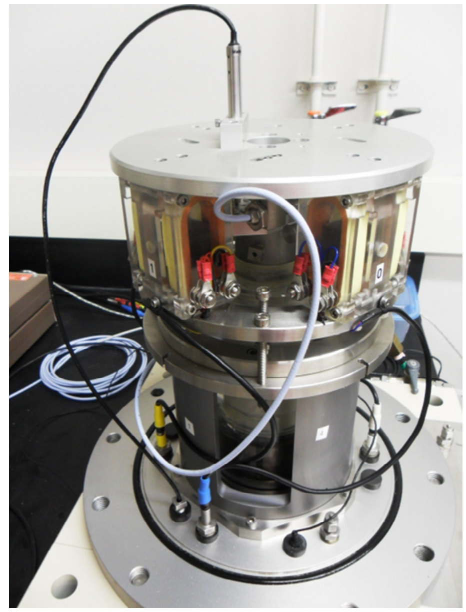

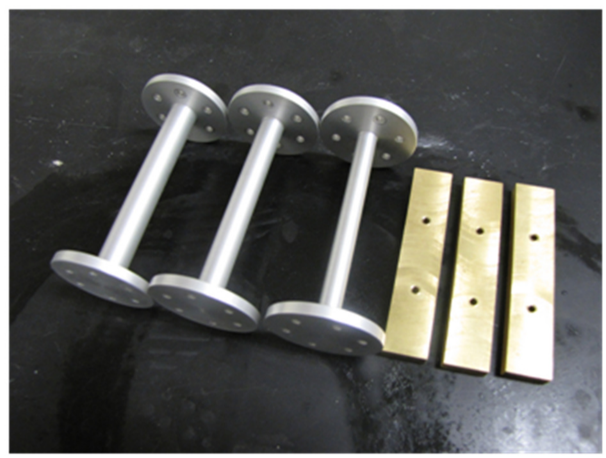

Figure 3. General instrumentation for resonant column device RCD-2

3 EXPERIMENTAL PROGRAM

To accurately measure the effect of the equipment on the test results, it is critical to ensure that the same testing procedures were used for both RCDs. While developing the testing procedure, practice tests are performed with all members of the testing teams present to ensure that samples would be prepared and tested similarly. Three aluminum specimens are used to calibrate the resonant-column systems. The aluminum specimens are made of a vertical aluminum pipe with two horizontal aluminum bars or disks. The bars or disks are attached at each end of the pipe to allow assemblage of the probe with the resonant column (Figures 4a, 4b). The main characteristics of the calibration specimens tested are given in Table 1.

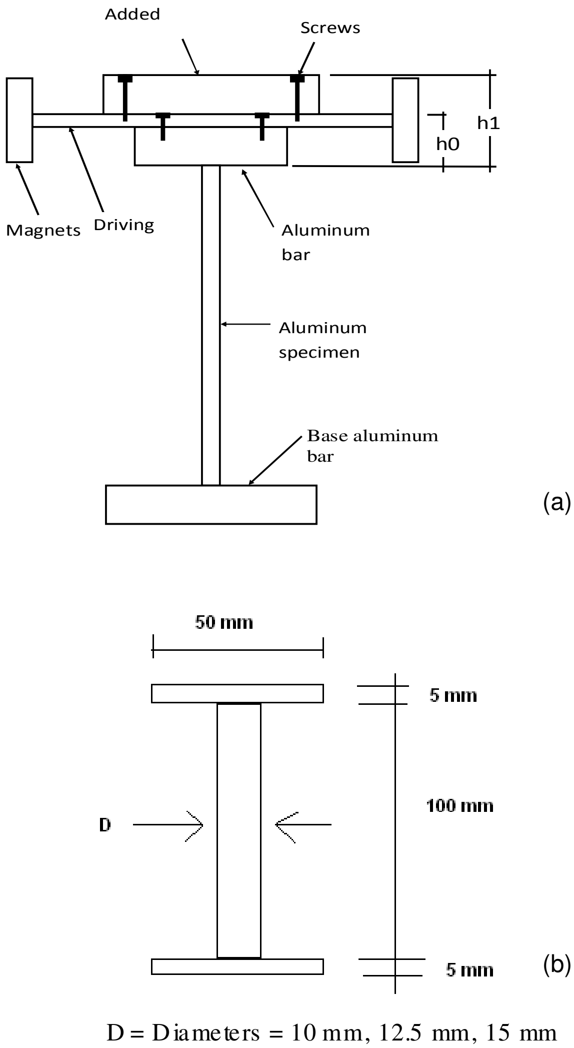

Figure 4. Calibration bar for systems a) RCD-1 and b) RCD-2.

Four different Ottawa sand specimens were tested in this study. Sands 1 and 2 (S1, S2) were tested in the RCD-1; whereas, sands 3 and 4 (S3, S4) were tested in the RCD-2. At each confinement and shear strain level, the dynamic properties were computed using the analytical procedures described before. To reduce the effects of large-strain cyclic loading, the specimens are compacted before testing to an average relative density D_R ≈ 77 %. The main characteristics of the sand specimens are given in Table 2.

All sand specimens were tested at confining pressures of 30, 60, 120, and 240 kPa, with 0 kPa back pressure. For each pressure, the resonant frequency and damping ratio were measured over a range of shear strains ($10^{-6} < \gamma < 10^{-3}$). Vertical displacements were measured throughout the tests and after unloading with the use of an LVDT. After unloading each sample, the residual vertical strain was required to be less than 0.2% to ensure that the samples did not change significantly throughout the testing.

Table 1. Characteristics of the aluminum probes

Device	Prob	Diameter (cm)		Length (cm)	Resonant Frequency (Hz)
		Outside	Inside		
RCD - 1	AL 1	0.955	0.701	22.54	12
RCD - 1	AL 2	2.534	1.901	22.54	97
RCD - 2	AL 3	1	0	10	40.7
RCD - 2	AL 4	1.5	0	10	90

Table 2. Change in height and void ratio during the test

Property of Specimen	S1	S2	S3	S4
Initial diameter D0 (mm)	69.97	70.32	50.17	49.84
Height during loading (mm)	146.44	144.23	97.69	96.56
Height after Unloading (mm)	146.47	144.14	97.61	96.55
Residual axial strain (%)	0.02	0.06	0.08	0.02
Void ratio during loading	0.521	0.496	0.531	0.561
Void ratio after Unloading	0.520	0.493	0.530	0.561
Max change in Void Ratio (%)	0.21	0.60	0.24	0.05
Average Density (kg/m3)	1741	1749	1736	1702

4 SAMPLE PREPARATION

Ottawa silica sand was chosen for testing because it is well characterised in the literature and is uniformly graded, which should enhance the reproducibility of samples. The geotechnical properties of the silica sand were determined in the laboratory; its grain size distribution is shown in Fig. 5 (D_{50}=0.279 mm, e_{max}=0.727, e_{min}=0.476, SiO^2 content 99.6% and Gs=2.66). Samples were prepared in a split mold by the dry pluviation and tamping technique. Once the upper platen was set in place, vacuum was applied to hold the sample and the split mold was removed. Then, connections for the driving plate, LVDT, and accelerometer were made, and the chamber was assembled. Sample vacuum was gradually released while increasing the cell pressure. Isotropic loading was applied to all samples tested in this study, increasing the confining pressure from 30 kPa to 240 kPa.

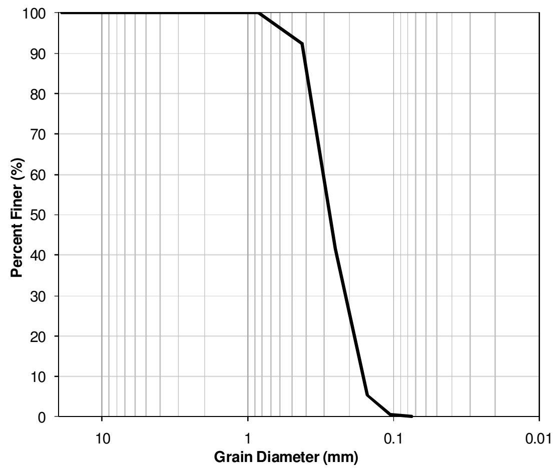

Figure 5. Grain size distribution of silica sand used (Barco sand #49)

The diameter of the cylindrical specimens for the RCD-1 is 70 mm; whereas the diameter is 50 mm for the RCD-2. All sand samples were tested in dry conditions. Each sample was built in five layers; each layer was tamped 70 times with a plastic tamper at a constant height. To achieve the same void ratio for both sample sizes, a tamper with a smaller tamping area was used for the 50 mm diameter samples than for the 70 mm diameter samples.

5 RESULTS AND DISCUSSIONS

Figure 6 shows the variation of damping ratio with shear strain level for the calibration specimens. The results for the low frequency probes at low strains levels (Fig. 6a, Table 1) indicate that the damping in the RCD-1 is 1.6 times larger than the damping measured with the RCD-2; and that the damping ratio increases almost linearly with the strain level. The damping ratio in aluminum specimens at the testing frequencies of the resonant column is practically zero (Zemanek, and Rudnick 1961); thus the observed increase in damping with strain level could be generated by the radiation of energy through the base of the resonant column. The base of the resonant column is assumed to be fixed; however, it has been demonstrated that for the evaluation of shear modulus the base is not perfectly fixed and a correction factor should be applied to the measured values especially for stiff specimens (Khan et al. 2008, Avramidis and Saxena 1990). The results for the high frequency probes (Fig. 6b) show an increase in the damping values measured with the RCD-1 compared to the corresponding values using the RCD-2 (5 times larger). This increase in attenuation confirms the non-fixed conditions of the base; as the stiffness ratio of the probes tested in the RCD-1 is 65; whereas, the ratio is equal to 5 for the RCD-2 probes. For the low and high frequency probes (Fig. 6), the damping measurements from the RCD-1 are higher than the measured values using the RCD-2 because different base fastening conditions. The RCD-1 is mounted on a flexible bench; whereas the RCD-2 is attached to a stiffer bench. The radiation damping in the RCD-1 increases with the increase the stiffness of the aluminium probe as expected. However, further studies are required to better characterize the radiation damping. The increase in radiation damping with shear strain and frequency is observed on aluminum probes because of their low damping in comparison with typical soils.

Figures 7 and 8 show typical results for the dynamic properties measured at σ'_o=30 and σ'_o=120 kPa. The results from the two devices are in good agreement. The maximum difference in damping ratio, at low strain levels, is 31%; whereas the maximum difference in the normalized shear modulus is 20%. The shear modulus is normalized to remove the effect of void ratio using the correction factor proposed by Hardin and Drnevich (1972). Table 3 shows that the difference in shear modulus and damping ratio for σ'_o=240 kPa are only 2% and 12% respectively. These differences could be related to the different sizes of the specimens and the coupling conditions between the top and bottom caps with the specimen. The platens of the RCD-2 provide better coupling conditions than those of the platens of the RCD-1 because they have deeper grooves. The difference in the damping ratios measured with the two systems is expected to increase with shear strain because of the different testing procedures used. However, these differences are not significant up to the maximum strain levels achieved in this study. The variation of shear modulus and damping ratio with shear strain level are in good agreement and follow the hyperbolic model (Fig. 9). Figure 9b shows typical results for the normalized values of the shear modulus with respect to G_{max}.

Table 3. Summary of Ottawa sand results for low shear strain levels ($2.7*10^{-6} < \gamma < 1.0*10^{-5}$)

Confinement (Kpa)	Sample	Void ratio	Resonanat frequency (Hz)	Damping (%)	Shear Velocity (m/s)	Shear Modulus (Gpa)	G /F(e)*
30	S1	0.521	48.9	0.71	176.1	54.3	30.3
30	S2	0.496	50.0	0.52	163.7	47.7	25.4
30	S3	0.532	48.3	0.49	179.9	56.2	32.1
30	S4	0.563	45.2	0.45	171.3	50.0	30.2
Difference Avg (%)		7.72	5.44	23.66	3.35	4.08	11.90
60	S1	0.521	57.1	0.42	205.8	74.1	41.4
60	S2	0.495	58.7	0.37	192.0	65.6	35.0
60	S3	0.532	61.1	0.72	227.6	89.9	51.4
60	S4	0.563	58.1	0.33	220.0	82.4	49.9
Difference Avg (%)		7.81	2.92	32.18	12.50	23.35	32.47
120	S1	0.520	69.3	0.29	249.5	108.9	60.8
120	S2	0.495	76.9	0.39	251.5	112.6	59.9
120	S3	0.533	73.3	0.60	273.1	129.4	73.9
120	S4	0.563	70.0	0.29	264.9	119.4	72.3
Difference Avg (%)		7.99	1.93	30.99	7.40	12.33	21.11
240	S1	0.520	92.8	0.27	334.1	195.3	109.0
240	S2	0.494	93.2	0.31	325.0	188.1	99.9
240	S3	0.533	87.9	0.44	327.4	186.1	106.3
240	S4	0.563	85.0	0.21	321.4	175.8	106.4
Difference Avg (%)		8.09	7.01	12.46	1.55	5.60	1.82

* $F(e) = (2.17 - e)^2 / (1 + e)$ Hardin and Drnevich (1972)

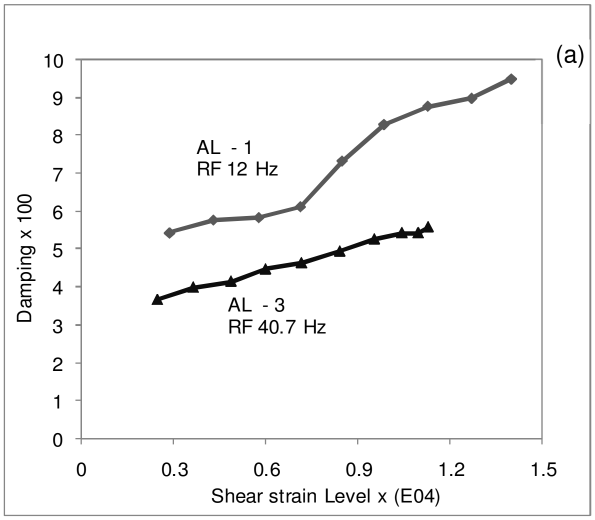

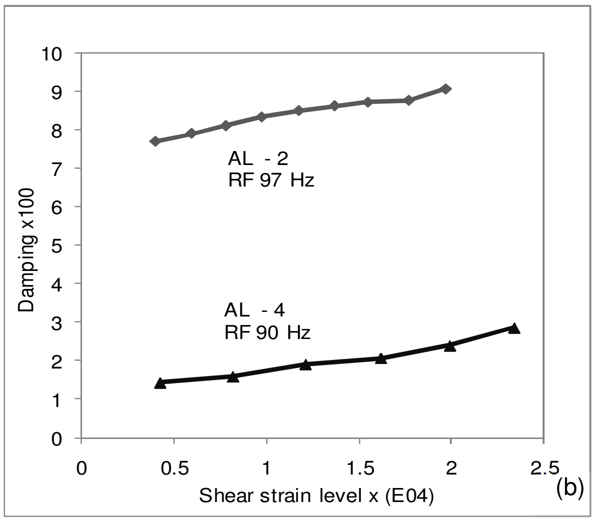

Figure 6. Damping vs. shear strain level for aluminum probes (a) low frequency, (b) high frequency

6 CONCLUSIONS

The results of an experimental study using two different resonant columns are presented. RC tests are performed on calibration aluminum probes and on dry sands (Ottawa silica sand). The results from the calibration probes show that the base of the RC cannot be considered fixed as the damping ratio increases with the excitation frequency. This trend suggests that radiation damping should be considered in the data analysis, especially at low strain levels where the damping ratio of the tested dry sands is smaller than 1%. The measured damping ratio of the aluminum probes differed by up to an order of magnitude for the different types of equipment used. The damping ratio and shear modulus at low strains measured with the two devices differed by up to 32% for the dry sand specimens. This difference could have been generated by the different coupling between the top caps and the specimens and also because of the different geometry of the specimens. However, the results are in good agreement with the predictions of the standard hyperbolic model once that the curves are normalized with respect to G_{max}.

7 ACKNOWLEDGEMENTS

This research is part of a study on non-destructive testing of geomaterials. Support is provided by the Natural Sciences and Engineering Research Council of Canada (NSERC), the University of Waterloo, and the University of Western Ontario. Gratitude is due to all of these funding agencies.

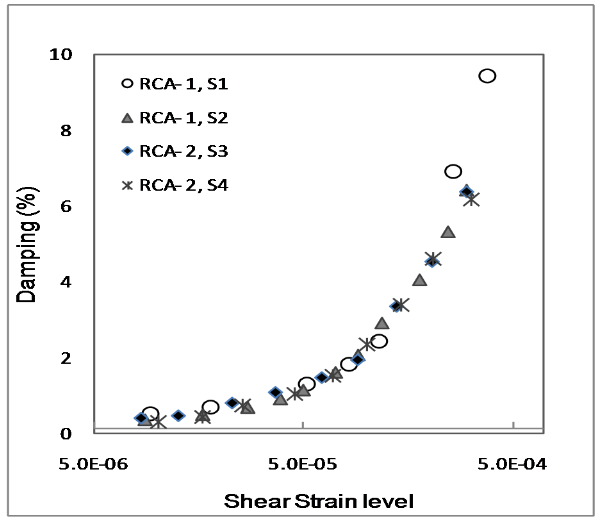

Figure 7a. Damping vs. log(shear strain level) σ' = 30 kPa

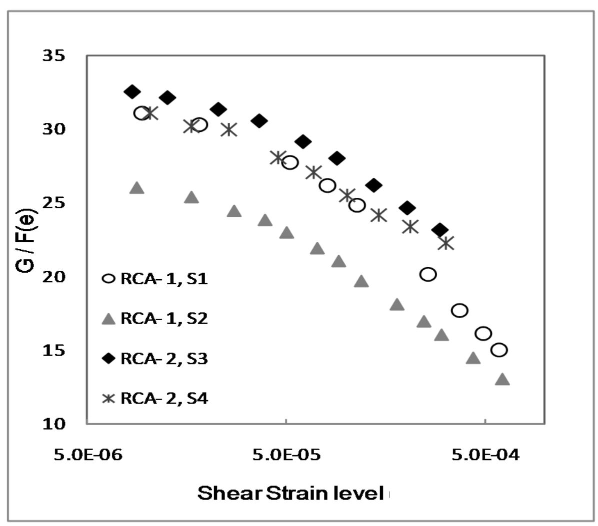

Figure 7b. Shear modulus vs. log(shear strain level) σ' = 30 kPa

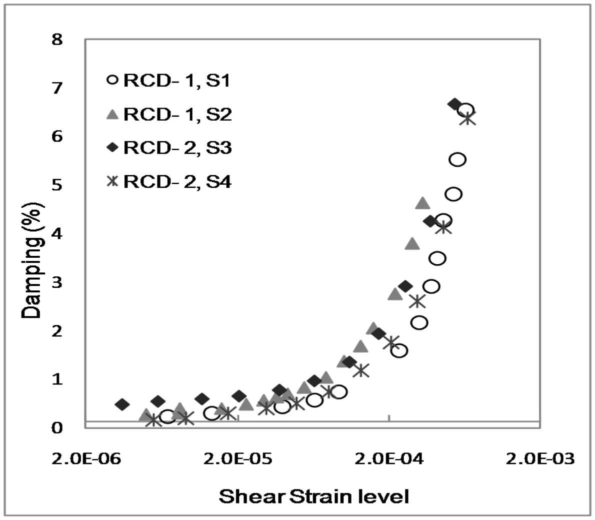

Figure 8a. Damping vs. Shear strain level
σ' = 120 kPa.

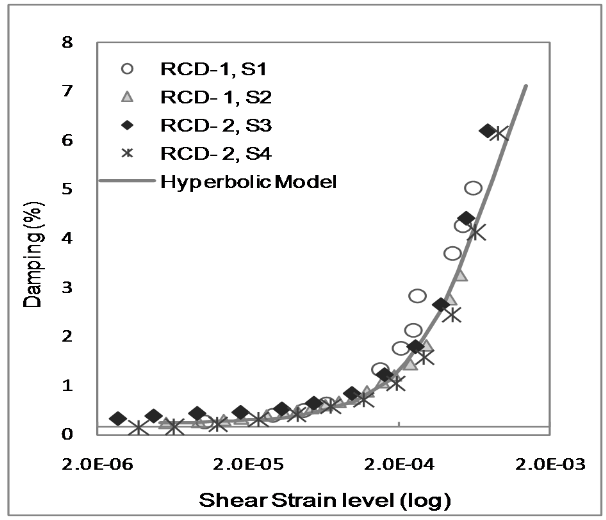

Figure 9a. Damping vs. shear strain level
σ' = 240 kPa.

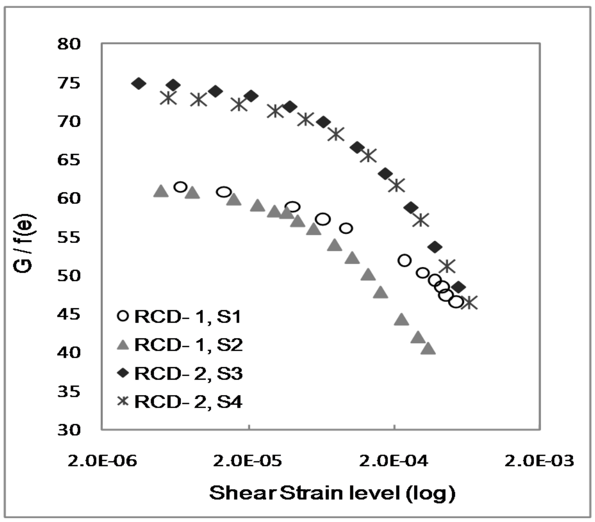

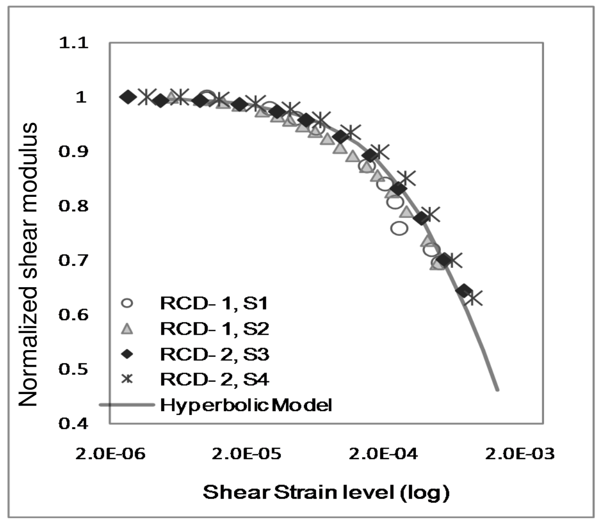

Figure 8b. Shear modulus vs. Shear strain level
σ' = 120 kPa.

8 REFERENCES

Avramidis, A.S. and Saxena, S.K. 1990. The Modified "Stiffened" Drnevich Resonant Column Apparatus. Japanese Society of Soil Mechanics and Foundation Engineering. Vol. 30, No. 3, 53-68.

Ashmavy, A.K., and Drnevich, V.P., 1994. "A General Dynamic Model for Resonant Column/Quasi-static Torsional Shear Apparatus", Geotechnical Testing Journal, ASTM, Vol. 17, No. 3, pp. 337-348.

ASTM D4015-92, 2000. "Standard Test Methods for Modulus and Damping of Soils by the Resonant-Column Method," American Society for Testing and Materials, Annual Book of Standards.

Bolton, M. D., and Wilson, J. M. R. 1989. An Experimental and Theoretical Comparison between Static and Dynamic Torsional Soil Tests. Géotechnique, 39(4), 585-599.

Booij, H. C., and Thoone, G. P. C. M. 1982. Generalization of Kramers-Krönig Transforms and Some Approximations of Relations between Viscoelastic Quantities. Rheologica Acta, 21, 15-24.

Camacho-Tauta, J.; Santos, J. A.; Ferreira, C. and Viana da Fonseca, A. 2008. Moving Windows Algorithm to Reduce Uncertainties in Bender Element Testing. XI Portuguese National Congress of Geotechnics, Portugese Society of Geotechnics, Coimbra, 149-156.

Cascante, G. and Santamarina, J. C. 1997. Low Strain Measurements Using Random Noise Excitation, Geotechnical Testing Journal, 20(1): 29-39.

Cascante, G., Santamarina, J.C., and Yassir, N., 1998. Flexural Excitation in a Standard Resonant Column Device. Canadian Geotechnical Journal, 35(3): 488-490.

Cascante, G., Vanderkooy, J., and Chung, W., 2003. Difference between current and voltage measurement in resonant column testing. Canadian Geotechnical Journal, 40(4): 806-820.

Christensen, R. M., 1971. Theory of Viscoelasticity – An Introduction. Academic Press, New York.

Drnevich, V. P., 1967. "Effects of strain history on the dynamic properties of sand," Ph.D. Thesis, University of Michigan, 151 pp.

Hardin, B.O. and Drnevich, V.P. 1972. Shear Modulus and Damping in Soils: Measurements and Parameter Effects. Journal of Soil Mechanics and Foundations Engineering, ASCE, 98(SM6): 603-624.

Hardin, B.O., 1965. The Nature of Damping in Sands. Journal of the Soil Mechanics and Foundations Division, ASCE, Vol. 91, No. SM1, pp. 63-97.

Iwasaki, T., Tatsuoka, F., and Takagi, Y. 1978. Shear Modulus of Sands under Cyclic Torsional Shear Loading. Soils and Foundations, 18(1), 39-56.

Khan, Z. H., Cascante, G., and El Naggar, M.H., 2008a. Linearity of the first torsional mode of vibration and base fixidity in resonant column. ASTM, Geotechnical Testing Journal, 31(1): 587 - 606.

Khan, Z. H., Cascante, G., El Naggar, M.H., and Lai, C. 2008b. Measurement of frequency-dependent dynamic properties of soils using the Resonant-Column device. Journal of Geotechnical and Geoenvironmental Engineering, ASCE, 134(9): 1319-1326.

Kim, D.-S., and Stokoe, K. H. 1995. Deformational Characteristics of Soils at Small to Medium Strains. Earthquake Geotechnical Engineering, Tokyo, Japan, 89-94.

Lovelady, P. L. and Picornell, M. (1990), "Sample coupling in resonant column testing of cemented soils." Dynamic Elastic Modulus Measureemnt in Materials, ASTM STP 1045, Philadelphia.

Richart F. E., Hall J. R. and Woods R. D. 1970. Vibrations of soils and foundations. Prentice Hall, Englewood Cliffs, pp: 414.

Rix, G. J., and Meng, J. 2005. A non resonance method for measuring dynamic soil properties., Geotechnical Testing Journal, 28(1), pp.1-8.

Stokoe, K.H. II, Hwang, S.K., Lee, J.N.-K, and Andrus, R.D. 1994. Effects of various parameters on stiffness and damping of soils to medium strains, Proceedings, International Symposium on Prefailure Deformation Characteristics of Geomaterials, Vol. 2, Japanese Society of Soil Mechanics and Foundation Engineering, Sapporo, Japan, September, 785-816.

Wang, Y.H., Cascante, G., and Santamarina, J.C. 2003. Resonant column testing: the inherent counter emf effect. Geotechnical Testing Journal, ASTM, 26(3): 342-352.

Woods, R.D., 1978, "Measurement of Dynamic Soil Properties", Proceedings, ASCE Specialty Conference on Earthquake Engineering and Soil Dynamics, Pasadena, California. Vol.1, pp. 91-178.Dobry, R. and Vucetic, M. (1987) State of the art report: Dynamic properties and response of soft clay deposits. Proc. Int. Symp on Geotechnical Engineering of Soft Soils, Vol. 2, 51- 87.

Zemanek, J., Jr., and Rudnick, I. 1961. Attenuation and dispersion of elastic waves in a cylindrical bar. The Journal of the Acoustical Society of America, 33: 1283-1288.